Influence of Harmonic Components in Traction System on the Traction Motor of High-speed Train

Xun Wang, Pingbo Wu*, Sheng Qu, Hao Wu

***Abstract*—AC-DC-AC traction transmission system provides power for high-speed train and is one of the key technologies for rail transit. The rectifier part adopts a four-quadrant rectifier, which has advantages such as high power factor, low harmonic content, and energy feedback. However, due to the power characteristics of single-phase power supply in electrified railways, there is a double power frequency fluctuation in the DC link voltage of the traction transmission system. In addition, the current output controlled by the inverter contains higher-order harmonics. In order to study the influence of harmonic components on the traction motor of high-speed train, an AC-DC-AC traction system simulation model for high-speed train was established. The results show that after LC filtering, at the condition that the stator current frequency is close to 100Hz, the motor stator current still undergoes distortion, but the effect on torque is not significant. When the LC filter fails, the torque ripple caused by 100Hz is very significant. It is recommended to consider this in the fault detection system of the traction transmission system. During train operation, the torque ripple at frequency of 6-times motor stator current is prominent, and this frequency also exists in the voltage and current of the DC link.**

***Index Terms*—High-speed train, Traction motor, DC link Voltage Fluctuation, Torque vibration**

I. Introduction

The AC-DC-AC traction transmission system [1-3] is widely used in electric traction systems for railway in China, mainly including transformer, single-phase pulse rectifiers, intermediate DC links, three-phase inverters, and traction motors, as shown in Fig. 1. The train receives power from the single-phase 25kV contact network through a pantograph, then depressurizes it through a power frequency transformer and inputs it into a single-phase pulse rectifier. The single-phase pulse rectifier rectifies and outputs stable DC voltage, which is input to the three-phase inverter through the DC link. The inverter generates three-phase AC voltage to drive the three-phase asynchronous traction motor [4-6], thereby achieving power output.

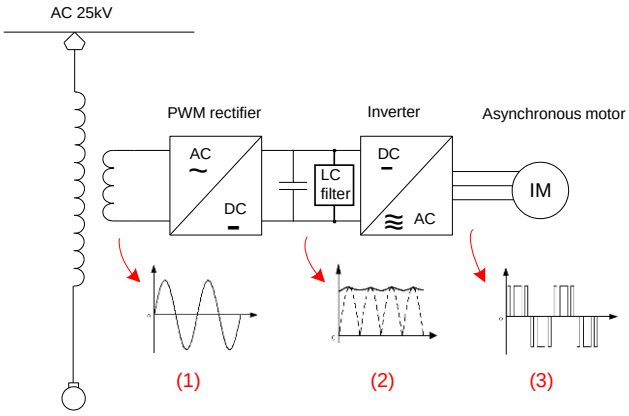

Fig. 1 Schematic diagram of the traction system for high-speed train.

In the AC-DC-AC traction system of high-speed trains, the DC voltage output by a single-phase pulse rectifier contains a pulsating component, which is twice the frequency of the power grid. This component can cause an increase in electromagnetic torque ripple and stator current distortion, known as beat frequency phenomenon [7-10]. When the operating frequency of the motor is close to the beat frequency voltage frequency, the beat frequency phenomenon is the most severe. At this point, a smaller beat frequency voltage would also generate a very large beat frequency current, causing problems such as rapid increase in motor power loss, rapid temperature rise, and severe fluctuations in electromagnetic torque, posing a serious threat to the safe operation of the train [11, 12]. At the same time, the three-phase AC output from the inverter contains a series of high-frequency harmonic components, which interact with the fundamental magnetic flux to form pulsating torque [13, 14]. Through the electromechanical coupling system, it would cause vibration fatigue problems in the mechanical system of high-speed trains.

Wu *et al.* [15] analyzed the influence of torque pulsation caused by voltage pulsation in the DC-link of traction drive system on motor hanger and studied the structural fatigue damage of the drive system. A method with Voltage Linear Interpolation Compensation for suppressing the beat frequency phenomenon was proposed by Song *et al.* [16],

Manuscript received August 10, 2023; revised April 26, 2024.

This work was supported gratefully by National Natural Science Foundation of China (U1934202, U2034210)

Xun Wang is a Ph.D. Candidate of State Key Laboratory of Rail Transit Vehicle System, Southwest Jiaotong University, Chengdu, Sichuan 610031, PR China. Email: wxptf0323@my.swjtu.edu.cn.

Pingbo Wu* is a Research Fellow of State Key Laboratory of Rail Transit Vehicle System, Southwest Jiaotong University, Chengdu, Sichuan 610031, PR China. Email: wupingbo@163.com

Sheng Qu is a Postdoctoral Researcher of State Key Laboratory of Rail Transit Vehicle System, Southwest Jiaotong University, Chengdu, Sichuan 610031, PR China. Email: 626193245@qq.com

Hao Wu is a Postdoctoral Researcher of College of Mechanical and Vehicle Engineering, Chongqing University, Chongqing 400044, PR China. Email: 438012650@qq.com

which is a Digital OCC Scheme. Ouyang *et al.* [17] improved compensation performance by using a repetitive DC link voltage predictor, which can significantly suppress steady-state beat current by several times. Diao *et al*. [18] used a ripple control scheme in vector control systems to reduce torque and current ripple amplitude, which compensates for slip frequency without the need for hardware filters. He *et al.* [19] used interdisciplinary research to improve switching frequency and mode selection by balancing torque, efficiency, and NVH performance of traction motor.

Double power frequency pulsation in the DC link would have an adverse impact on the control performance of the four-quadrant converter and traction motor [20]. Based on the AC-DC-AC traction system simulation model, the influence of harmonics on traction motor and their mutual influence in traction systems were investigated. The acceleration, uniform speed, and braking processes of train operation were simulated, and the results were analyzed by using short-time Fourier transform in this study.

II. Motor Voltage and Torque Analysis under DC Link Voltage Fluctuation

Pulse width modulation technology is used for inverter in traction drive systems. If only basic components are considered, the switch function is represented as [17]

$$\begin{bmatrix} S_a \\ S_b \\ S_c \end{bmatrix} = \begin{bmatrix} u_a^*(t) \\ u_b^*(t) \\ u_c^*(t) \end{bmatrix} / \frac{U_d}{2} = \begin{bmatrix} U_{1m}\sin(\omega_1 t) \\ U_{1m}\sin(\omega_1 t - \frac{2\pi}{3}) \\ U_{1m}\sin(\omega_1 t + \frac{2\pi}{3}) \end{bmatrix} / \frac{U_d}{2} \tag{1}$$

Where, $u_a^*(t), u_b^*(t), u_c^*(t)$ are output phase voltages, U_d is DC voltage, U_{1m} is amplitude of the output voltages, ω_1 is angular frequency of output voltages. Assuming there is a fluctuating component in DC voltage, the DC voltage could be expressed as

$$u_d(t) = U_d + U_r \sin(\omega_r t + \theta_r) \tag{2}$$

Where, U_r, θ_r and ω_r are amplitude, phase, and angular frequency, respectively.

The available output voltage is

$$\begin{bmatrix} u_a \\ u_b \\ u_c \end{bmatrix} = \begin{bmatrix} S_a \\ S_b \\ S_c \end{bmatrix} \cdot \frac{u_d(t)}{2} \tag{3}$$

From Eq. 4, it can be seen that the output phase voltage of the inverter consists of three components. The latter two components are formed by modulating the fluctuation component through the inverter. If there are more fluctuation components in the system, there would also be more harmonic frequencies in the output voltage.

Where $m = 2U_{1m} / U_d$, the output voltage of phase a is represented as

$$\begin{aligned} u_a(t) &= S_a \cdot \frac{u_d(t)}{2} = m\sin(\omega_1 t) \cdot \frac{U_d + U_r \sin(\omega_r t + \theta_r)}{2} \\ &= U_{1m}\sin(\omega_1 t) + m \cdot \frac{U_r}{2}\sin(\omega_1 t)\sin(\omega_r t + \theta_r) \\ &= U_{1m}\sin(\omega_1 t) + m \cdot \frac{U_r}{4}\cos[(\omega_r - \omega_1)t + \theta_r] \\ &\quad - m \cdot \frac{U_r}{4}\cos[(\omega_r + \omega_1)t + \theta_r] \end{aligned} \tag{4}$$

When the output voltage frequency approaches the fluctuation frequency, the beat frequency ($\omega_r - \omega_1$) could be small, however, it could still form a large beat current, causing torque ripple of the traction motor.

According to PWM rectification theory, ignoring the loss of rectifier power devices and the equivalent impedance of transformer secondary side, the output power is equal to the input power, and the DC side voltage ripple component could be obtained as follows

$$u_{dc} = \frac{I_L \sin(2\omega_s t + \phi)}{2\omega_s C_d \cos(\phi)} \tag{5}$$

Where, ω_s —Grid side angle frequency, ϕ —Phase angle of grid side current lead voltage, I_L —Average value of load current. From Eq. 5, it can be found that after PWM rectification, there is a component of twice the grid frequency (f_s =50Hz) in the DC link, which is 100Hz.

When the frequency of harmonic magnetic flux and harmonic rotor current is different, their interaction would generate vibration harmonic torque. For example, the instantaneous torque value generated by the stator current of the 5th harmonic current and the fundamental magnetic flux in each phase of the motor is

$$\begin{aligned} T_{A5-1} &= \frac{n_p}{2\pi f_1}\sqrt{2}I_{25}\sin(5\omega_1 t - \phi_2)\sqrt{2}E_2 \sin\omega_1 t \\ T_{B5-1} &= \frac{n_p}{2\pi f_1}\sqrt{2}I_{25}\sin\left[(5\omega_1 t - \phi_2) + \frac{2\pi}{3}\right]\sqrt{2}E_2 \sin\left(\omega_1 t - \frac{2\pi}{3}\right) \\ T_{C5-1} &= \frac{n_p}{2\pi f_1}\sqrt{2}I_{25}\sin\left[(5\omega_1 t - \phi_2) - \frac{2\pi}{3}\right]\sqrt{2}E_2 \sin\left(\omega_1 t - \frac{4\pi}{3}\right) \end{aligned} \tag{6}$$

Where, f_1 is fundamental voltage frequency of motor stator, n_p —number of pole pairs.

Using trigonometric relationships: $\sin\alpha\sin\beta = \frac{1}{2}\left[\cos(\alpha-\beta) - \cos(\alpha+\beta)\right]$, the vibration harmonic torque generating by the 5th harmonic current could be obtained by adding the torque of three phases

$$T_{5-1} = \frac{3n_p}{2\pi f_1} I_{25}E_2 \cos(6\omega t - \phi_2) = \frac{3n_p}{2\pi f_1} I_{25}E_2 \cos(6\omega t + \pi - \phi_2) \tag{7}$$

Similarly, the vibration harmonic torque generated by the 7th harmonic current is

Eq. 7 and Eq. 8 indicate that the 5th and 7th stator current harmonics generate a vibration torque of 6 times the stator

voltage fundamental frequency during the operation of the traction motor.

$$T_{7-1}=\frac{3n_{\mathrm{p}}}{2\pi f_1}I_{27}E_2\cos(6\omega t-\phi_2) \tag{8}$$

In turn, the vibration torque formed by the voltage ripple component of the DC link could be obtained

$$T_d=\frac{3n_{\mathrm{p}}}{2\pi f_1}I_{2d+}E_2\cos(\omega_r t-\phi_d)+\frac{3n_{\mathrm{p}}}{2\pi f_1}I_{2d-}E_2\cos(\omega_r t+\pi-\phi_d) \tag{9}$$

From Eq. 5, it can be seen that the DC link contains a pulsating component that is twice the grid frequency, i.e., $\omega_r=2\omega_s$.

III. Results and Discussion

The modeling illustration of the traction system is shown in Fig. 2. Based on the principles of transient current control and direct torque control, models were established for PWM rectifiers and traction inverters [21, 22].

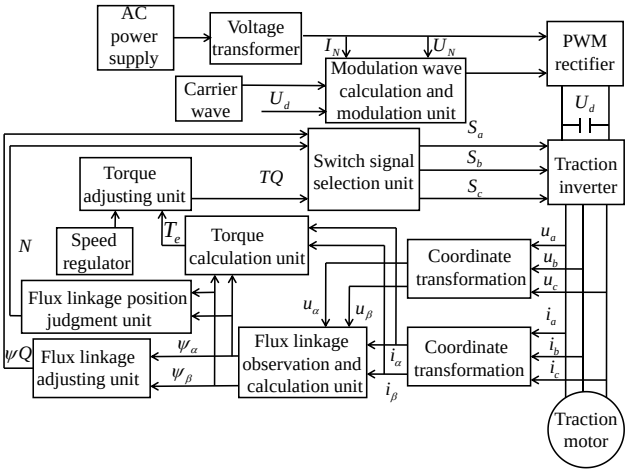

Fig. 2 Block diagram of traction system model for high-speed train.

Transient direct current control could achieve voltage stabilization, voltage regulation, unit power factor, and stable switching for working state in the rectifier link through voltage and current double closed-loop control. Its expression is as follows

$$\begin{cases} I_{N1}^*=K_P\left(U_d^*-U_d\right)+1/K_i\int\left(U_d^*-U_d\right)dt \\ I_{N2}^*=I_dU_d/U_N \\ I_N^*=I_{N1}^*+I_{N2}^* \\ u_{ab}(t)=u_N(t)-\left(\omega L_N I_N^*\cos\omega t+I_N^*R_N\sin\omega t\right)-K\left[I_N^*\sin\omega t-i_N(t)\right] \end{cases} \tag{10}$$

Where, K_P and K_i are the proportional and integral coefficients of the voltage loop PI controller, respectively. K is the proportional coefficient of the current inner loop.

Direct torque control uses the space vector analysis method to directly control the stator flux and electromagnetic torque by stator field orientation. In order to achieve feedback control in direct torque control systems, it is necessary to accurately estimate the current stator flux and torque. The estimation of stator magnetic flux of traction motor is as follows

$$\begin{cases} \psi_{s\alpha}=\int(u_{s\alpha}-i_{s\alpha}R_s)dt \\ \psi_{s\beta}=\int(u_{s\beta}-i_{s\beta}R_s)dt \end{cases} \tag{11}$$

According to the vector equation of asynchronous motors, the electromagnetic torque can be expressed as

$$T_e=n_{\mathrm{p}}\vec{\psi}_s\times\vec{i}_s \tag{12}$$

Observations of electromagnetic torque can be obtained as follows

$$T_e=n_{\mathrm{p}}(\hat{\psi}_{s\alpha}i_{s\beta}-\hat{\psi}_{s\beta}i_{s\alpha}) \tag{13}$$

Where, R_s is the stator resistance, n_{p} is the number of poles. $\vec{\psi}_s$ and $\vec{i}_s$ represent the stator flux space vector and stator current space vector under the three-phase shaft system, respectively. $\hat{\psi}_{s\alpha}$ and $\hat{\psi}_{s\beta}$ are estimated values, $i_{s\beta}$ and $i_{s\alpha}$ are measured values.

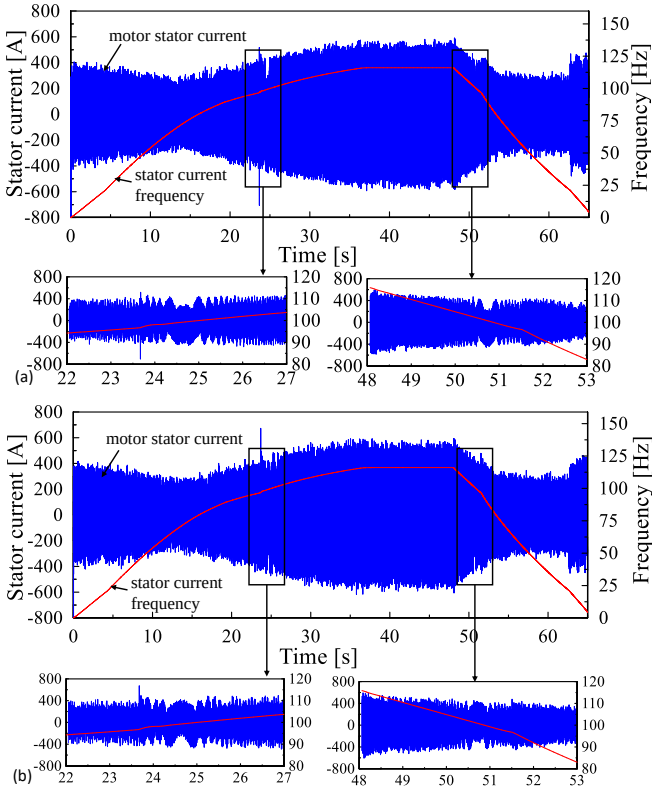

Fig. 3 Time diagram of traction motor stator current at full speed, (a) DC link with LC filter, (b) DC link without LC filter.

The simulation model of the traction system for high-speed train was established with Simulink module as in Matlab package, and the influence of the DC link voltage fluctuation on the stator current and torque of the traction motor was analyzed. Simulations were conducted at the presence or absence of an LC filter in the DC link at full speed. The motor speed was set to accelerate from 0 to 367 rad/s, run at a

constant speed for 10 seconds, and then decelerate.

Time diagram of traction motor stator current at full speed is shown in Fig. 3, and the 100Hz is the pulsating component that occurs after PWM rectification. In the enlarged image of Fig. 3, the phenomenon of current distortion exists in the stator current during the traction and braking stages, when the stator current frequency of the traction motor approaches 100Hz, and the distortion is most severe when the stator current frequency is equal to 100Hz. From Fig. 3, it can be found that regardless of the presence or absence of LC filter in the DC link, when the stator current frequency of the traction motor approaches 100Hz, distortion of the stator current would occur. It indicated that even if the 100Hz component of the DC link is filtered, it can still cause stator current distortion. Comparing Fig. 3(a) and Fig. 3(b), it can be found that when the DC link is equipped with LC filter, the stator current fluctuation is smaller than that without LC filter, indicating the necessity of DC link filtering.

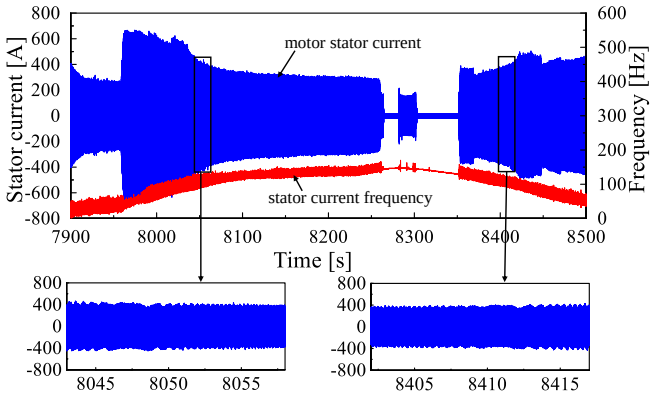

Fig. 4 Time diagram of stator current of traction motor based on line test data.

The current time-domain diagram of the traction motor of line test is shown in Fig. 4, where blue represents current and red represents current frequency. This time-domain diagram includes traction and braking conditions, both of which have passed through the current frequency of 100Hz, as shown in the enlarged part of the diagram. It can be observed that when the current frequency of the traction motor approaches 100Hz, i.e. $2f_s$, the current would undergo distortion, which is consistent with the simulation results in Fig. 3. It is indicated that the simulation model could effectively simulate this phenomenon.

The Short-time Fourier transform (STFT) was used in this work to detect changes in the frequency and time domain of the simulation results, and time frequency diagram of stator current of traction motor is shown in Fig. 5. In Fig. 5(b), the stator current has three distinct frequencies that vary with motor speed, namely fundamental frequency, harmonic frequency $5f_1$ and $7f_1$ due to PWM inverter. Meanwhile, the stator current has other two harmonic components with the frequencies of f_1-2f_s and f_1+2f_s due to DC voltage pulsations. The frequencies of $5f_1\pm2f_s$ and $7f_1\pm2f_s$ exist in stator current, but the amplitudes of which are smaller than that of $f_1\pm2f_s$. After the DC link is filtered by LC, in Fig. 5(a), the harmonic components caused by DC voltage fluctuation are not significant in the time frequency, but harmonic components caused by PWM inverter are still prominent.

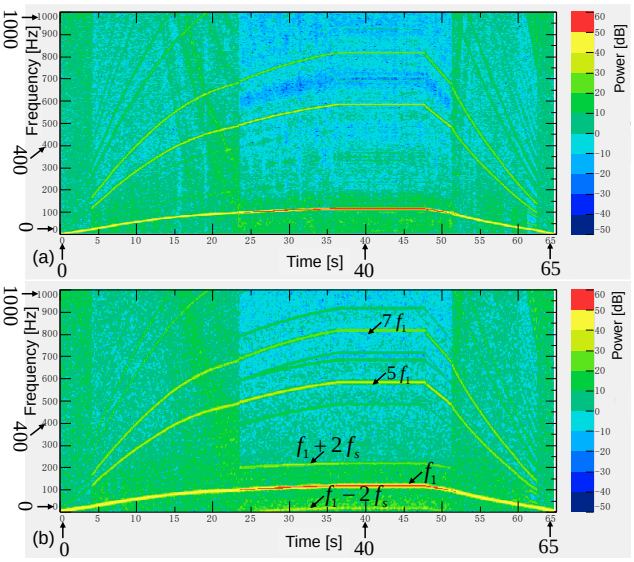

Fig. 5 Time frequency diagram of stator current of traction motor, (a) DC link with LC filter, (b) DC link without LC filter.

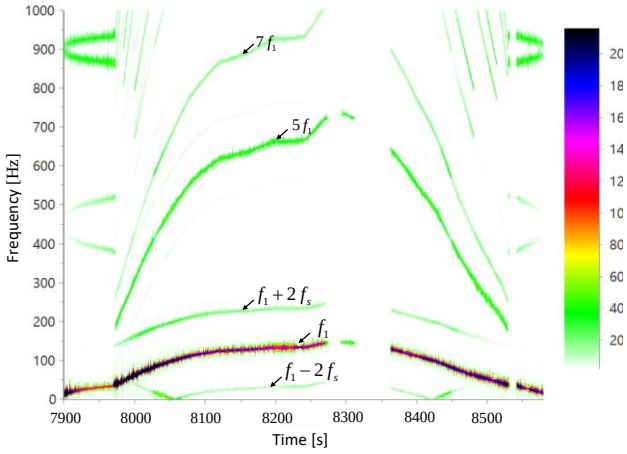

Fig. 6 Time frequency diagram of stator current of traction motor based on line test data.

The time-frequency diagram obtained from the short-time Fourier transform of the traction motor current in the line test is shown in Fig. 6. Several significant frequency bands that vary with speed in the fig. 6 are consistent with the simulation results in Fig. 5(b). The results of the line test were obtained from the poor filtering effect of the DC-link in the traction drive system, so prominent frequency bands f_1-2f_s and f_1+2f_s can be found, which are formed by the modulation of the f_1 and $2f_s$ components.

Fig. 7 shows the time frequency diagram of the torque of traction motor. In the spectrogram of Fig. 7(b), there is a remarkable harmonic component with the frequency of 100Hz, which is caused by DC link voltage fluctuation. In addition, there is also a harmonic component with frequency of $6f_1$ that varies with speed, which is caused by PWM inverter, as is mentioned previously. After f_1 is close to 100Hz, the vibration frequency 100Hz is more profound.

Compared with Fig. 7(b), it shows that only the harmonic component with frequency $6f_1$ is particularly prominent, indicating that after LC filtering in the DC link, the impact of 100Hz on the motor torque is significantly reduced. The harmonic components with frequency $6f_1$ and 100Hz would cause vibrations on the vehicle's mechanical system through electromechanical coupling.

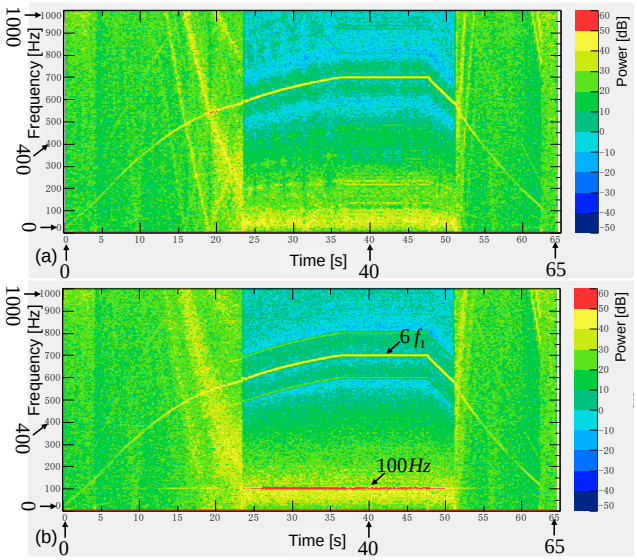

Fig. 7 Time frequency diagram of the torque of traction motor, (a) DC link with LC filter, (b) DC link without LC filter.

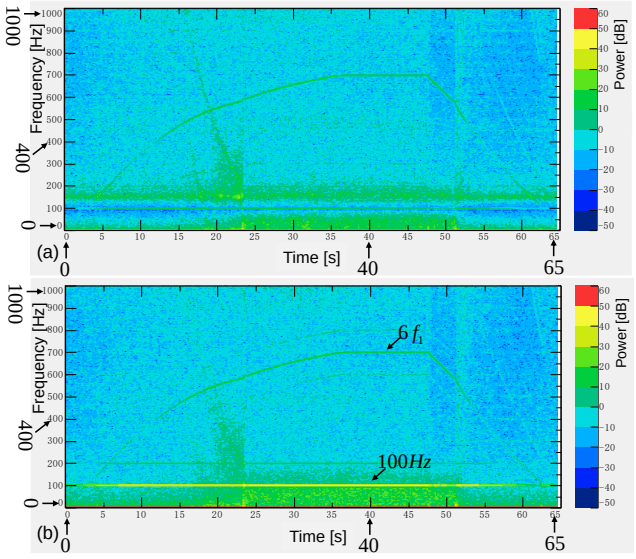

Fig. 8 Time frequency diagram of DC link voltage of traction system, (a) DC link with LC filter, (b) DC link without LC filter.

In Fig. 8, time frequency diagram of DC link voltage shows that harmonic component with frequency $6f_1$ exists in DC link voltage, which is caused by PWM inverter. This indicates that the harmonic torque frequency formed by the stator harmonic current and magnetic flux of the motor would affect the DC voltage through the inverter. In addition, two times the power frequency, i.e., 100Hz, exists in the DC link voltage, regardless of whether the LC filter is present or not. Compared with Fig. 8(b), Fig. 8(a) shows that the amplitude of 100Hz is significantly smaller, indicating that the LC filter has a significant filtering effect at 100Hz.

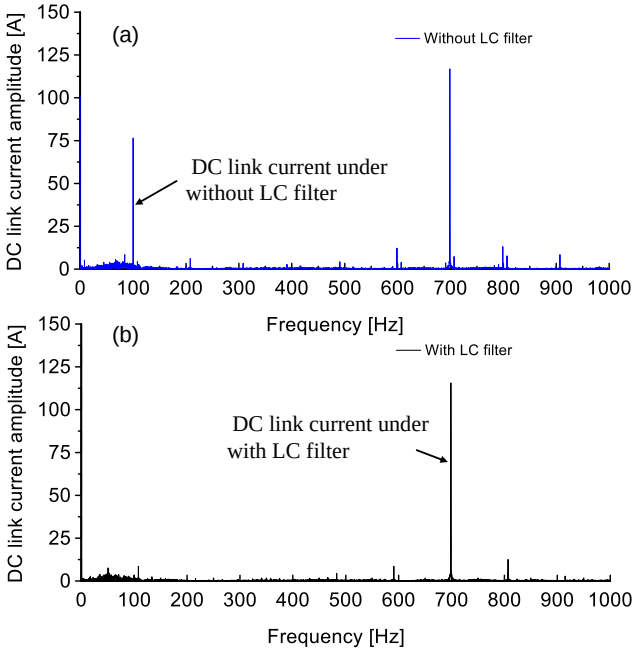

Fig. 9 Frequency domain diagram of DC link current of traction system.

The frequency domain diagram of DC link current during a constant speed operation period at w=367rad/s is shown in Fig. 9. Regardless of whether there is an LC filter or not, there is a harmonic frequency of 6 times the motor stator current fundamental frequency in the frequency domain of the DC link current, and the amplitude is basically the same. When the DC link without LC filter, 100Hz is prominent in the spectrum of the DC link current, indicating that the LC filter can effectively filter out the pulsation of 100Hz.

IV. Conclusions

In the AC-DC-AC traction transmission system, the DC voltage output by the single-phase rectifier has a pulsating voltage with a frequency twice that of the grid side voltage. When the stator current frequency of the traction motor is around 2-times the grid frequency, this pulsating voltage would cause current distortion and threaten the safe and stable operation of the train. In this paper, the simulation model of the traction system for high-speed train was established. The results reproduced the phenomenon of motor stator current distortion caused by pulsating voltage in the DC link, and found that harmonics at twice the grid frequency had a significant impact on motor torque without LC filter in DC link. The fault detection design of high-speed train traction drive system would consider the case of 100Hz filtering failure. In addition, the harmonic torque frequency formed by the stator harmonic current and magnetic flux of the motor would significantly affect the DC link through the inverter.

References

[1] Li L., Wu M., Wu S., et al. (2019) A Three-Phase to Single-Phase AC-DC-AC Topology Based on Multi-Converter in AC Electric Railway Application[J]. IEEE Access 7: p. 111539-111558.

[2] Tan M., He D., Wen J., et al. (2019) Influence of electric traction system on power grid harmonics. in IOP Conference Series: Materials Science and Engineering.
[3] Tanta M., Monteiro V., Exposto B., et al. (2017) Simplified rail power conditioner based on a half-bridge indirect AC/DC/AC Modular Multilevel Converter and a V/V power transformer. in Proceedings IECON 2017 - 43rd Annual Conference of the IEEE Industrial Electronics Society. p. 6431-6436.
[4] Wang X., Peng T.F., Wu P.B., Cui L.T. (2021) Influence of electrical part of traction transmission on dynamic characteristics of railway vehicles based on electromechanical coupling model[J]. Scientific Reports 11(1).
[5] Ma X., Ren J., Ge Q., Li Y. (2010) Digital control of four-quadrant PWM rectifier for high speed railway traction converter. in 2010 International Conference on E-Product E-Service and E-Entertainment, ICEEE2010.
[6] Wang H. and Wu M. (2015) Simulation analysis on low-frequency oscillation in traction power supply system and its suppression method[J]. Dianwang Jishu/Power System Technology 39(4): p. 1088-1095.
[7] Li Z., Xia J., Gao X., et al. (2023) Modulated Model Predictive Torque Control for Fault-Tolerant Inverter-Fed Induction Motor Drives With Single DC-Link Voltage Sensor[J]. IEEE Transactions on Power Electronics 38(7): p. 8798-8810.
[8] Wu X., Li K., Yu T., et al. (2023) A Capacitance Estimation Method for DC-Link Capacitors Based on Pre-Charging Model and Noise Evaluation[J]. IEEE Transactions on Industrial Electronics 70(8): p. 8477-8487.
[9] Zar T., Suan Tial M.K., Naing T.L. (2023) DC-link voltage balancing and control of qZ-source inverter fed induction motor drive[J]. International Journal of Electrical and Computer Engineering 13(4): p. 3733-3746.
[10] Zhang R., Yin Z., Zhan Z., Yu S. (2023) DC-link oscillation suppression method based on q-axis voltage compensation of a 180 kW PMSM traction system for urban rail transit[J]. Energy Reports 9: p. 323-331.
[11] Guenter S., Yang J., Buticchi G., et al. (2023) DC-Link Voltage Dynamics of Three-Level Four-Wire Grid-Connected Converters during Harmonics Injection Operations[J]. IEEE Transactions on Industrial Electronics 70(8): p. 8000-8008.
[12] Yin J., He X., Lu J., Chung H.S.H. (2023) Phase-Shift Control With Unified PWM/PFM for Improved Transient Response in a Bidirectional Dual-Active-Bridge DC/DC Converter[J]. IEEE Transactions on Industrial Electronics 70(9): p. 8862-8872.
[13] Kim Y.S. (2022) Analysis of Current Harmonics and Torque Characteristics according to Winding Connection of BLDC Motor for Railway Vehicle Door Control[J]. Transactions of the Korean Institute of Electrical Engineers 71(10): p. 1420-1426.
[14] Lu B., Liu Z., Wang X., et al. (2023) Influence of Electric Traction Drive System Harmonics and Interharmonics on the Vibration of Key Locomotive Components[J]. IEEE Transactions on Vehicular Technology: p. 1-16.
[15] Wu P.B., Guo J.Y., Wu H., Wei J. (2021) Influence of DC-link voltage pulsation of transmission systems on mechanical structure vibration and fatigue in high-speed trains[J]. Engineering Failure Analysis 130.
[16] Song Y., Song W., Yu B. (2019) Digitized Implementation of Beat-frequency Suppression Algorithm Based on One-cycle Control for Traction Motors[J]. Zhongguo Dianji Gongcheng Xuebao/Proceedings of the Chinese Society of Electrical Engineering 39(10): p. 3007-3015.
[17] Ouyang H., Zhang K., Zhang P., et al. (2011) Repetitive compensation of fluctuating DC link voltage for railway traction drives[J]. IEEE Transactions on Power Electronics 26(8): p. 2160-2171.
[18] Diao L.J., Dong K., Yin S.B., et al. (2016) Ripple analysis and control of electric multiple unit traction drives under a fluctuating DC link voltage[J]. Journal of Power Electronics 16(5): p. 1851-1860.
[19] He S., Gong C., Zhang P., et al. (2023) Analysis and Validation of Current Ripple Induced PWM Switching Noise and Vibration for Electric Vehicles. in SAE Technical Papers.
[20] Kapila M. Warnakulasuriya, Gayashan P., et al. (2022) Artificial Intelligence-based Design Approach to Magnetics. Lecture Notes in Engineering and Computer Science: Proceedings of The World Congress on Engineering 2022, 6-8 July, 2022, London, U.K., pp83-88.
[21] Lijian J., Wenhui Z., et al. (2022) Vibration Suppression of Flexible Joints Space Robot based on Neural Network. IAENG International Journal of Applied Mathematics, vol. 52, no.4, pp776-783.
[22] Cheng Z., Yu L., et al. (2022) RBFNN Fault Diagnosis Method of Rolling Bearing Based on Improved Ensemble Empirical Mode Decomposition and Singular Value Decomposition. IAENG International Journal of Computer Science, vol. 49, no.3, pp616-627.